

Original papers

GT-RootS: An integrated software for automated root system measurement from high-throughput phenotyping platform images

Philippe Borianne^{a,b,*}, Gérard Subsol^c, Franz Fallavier^{a,b}, Audrey Dardou^{d,e}, Alain Audebert^{d,e}

^a CIRAD, UMR AMAP, F-34398 Montpellier, France

^b AMAP, Univ Montpellier, CIRAD, CNRS, INRA, IRD, Montpellier, France

^c LIRMM, Univ Montpellier, CNRS, Montpellier, France

^d CIRAD, UMR AGAP, F-34398 Montpellier, France

^e AGAP, Univ Montpellier, CIRAD, INRA, INRIA, Montpellier SupAgro, Montpellier, France

ARTICLE INFO

Keywords:

Image processing pipeline
Root system architecture
Phenotyping platform

ABSTRACT

GT-RootS (*Global Traits of Root System*) is an automated Java-based open-source solution we are developing for processing root system images provided by the Rhizoscope, a CIRAD phenotyping platform dedicated to dense cereal plants. Two types of use are proposed. The fully-automated mode applies a predefined standard processing pipeline to a preselected set of images while the semi-automated mode allows the user to interactively check and correct intermediate processing results to a specific image. In both cases, GT-RootS combines a local adaptive thresholding algorithm and a similarity indicator to automatically separate the root system from a complex background without user intervention. A covering house-shaped polygon is then defined in the axis system of the root ellipse from vertical weighted density profiles. This canonical shape is composed of both upper trapezoid and lower rectangular compartments from which upper and lower heights, global width and local offset, root system cone angulation and spatial densities can be easily evaluated and displayed. GT-RootS measurements were compared both to expert evaluations and to two other estimation methods on a set of 64 images of a dense Japonica rice root system of 30-days-old plants. We demonstrate also that GT-RootS satisfies the requirements of high-throughput analyses: short processing time (around 30 images per hour on a low-end computer), measurement accuracy and repeatability, and user bias eradication.

1. Introduction

Cereal crop production is likely to decline with global warming (Parry et al., 2004; Lesk et al., 2016). This is especially true for rice due to its shallow rooting. Genetic improvement of its drought tolerance by deep and efficient rooting for better access to groundwater resources is a major challenge.

Understanding and measuring the adaptation of plants to their environment is based on high-throughput plant phenotyping approaches (Araus and Cairns, 2014; Granier and Vile, 2014) developed for studying the relationships between plant traits and the genome. These approaches lie behind the development of many phenotyping platforms which more often use various non-invasive sensors (Li et al., 2014; Humplík et al., 2015) such as visible red-green-blue (RGB) imaging, chlorophyll fluorescence imaging (CFIM), thermo-imaging or hyperspectral imaging. These phenotyping platforms are usually focused on shoot growth (Skirycz et al., 2011; Tisné et al., 2013; Mathieu et al., 2015) and/or root growth (Iyer-Pascuzzi et al., 2010; Clark et al., 2013;

Adu et al., 2014).

Plant root studies are a major challenge in the context of climate change; roots enable nutrient and water uptake and are thus crucial components of overall plant productivity (Gregory et al., 2009; Comas et al., 2014).

The shape and spatial arrangement of a root system are classically described by the *Root System Architecture* (RSA) (Kochian, 2016). RSA is created by modulating the growing and/or insertion angles, the rate of growth and type of individual roots contributing to the root system and varying between species, and also within species, in relation to genotype and the environment (Lynch, 1995). RSA is shaped by interactions between genetic and environmental components that establish a framework with which the plant explores the soil and responds to external cues that dictate future growth patterns.

Using digital imaging software to automate phenotypic analysis is an efficient way of accurately and reproducibly estimating the physiological traits of plants (Brewer et al., 2006; Wang et al., 2009; Das et al., 2015; Colombi et al., 2015).

* Corresponding author at: CIRAD, UMR AMAP, F-34398 Montpellier, France.
E-mail address: philippe.borianne@cirad.fr (P. Borianne).

At least forty image processing software packages concerning root system measurement have been proposed depending on various objectives, methods and equipment (Kuijken et al., 2015). They can be categorized by their dedicated domain – *2D or 3D root systems, anatomy of cross-sections,...* – level of automation – *manual, semi-supervised or fully automated* –, the nature of the main root traits they can estimate – *length and diameter, shape, architecture, elongation and growth,...* –, their availability and their distribution licence – *free or share-ware, on-demand, open-source or owner,...* They are mostly not dedicated to specific image processing and remain more or less adaptable. Some software packages propose a generic image processing pipeline defined for some particular tasks, whereas others are specifically designed for the phenotyping platform taking into account sensor specificities or acquisition methods. In this last case, better integration is achieved in the phenotyping process, leading to more precise or robust results and optimizing the processing time.

Our work addresses the processing of images provided by the Rhizoscope, a specific high-throughput root system phenotyping platform developed by CIRAD for understanding the adaptation mechanisms of root system architecture under environmental constraints (Audebert et al., 2010). We could presumably parameterize the *EZ-Rhizo* (Armengaud et al., 2009), *GiA Roots* (Galkovskyi et al., 2012) or *RootReader2D* (Clark et al., 2013) semi-automated software packages. However, Rhizoscope's images present some specificities which may prevent these software packages from giving significant results, especially (i) the non-uniform noise of pictures induced by the lighting source, (ii) the physical light diffraction properties in the Plexiglas pin grid or (iii) the root system density which prohibits root-axis recognition and the usual root architecture measurement. Software packages such as *RootNav* (Pound et al., 2013), *RootScape* (Ristova et al., 2013), *Aria* (Pace et al., 2014) and *GLO-RIA* (Rellán-Álvarez et al., 2015) evaluate spatial root development through simple shape indices and/or characterization by the convex hull to estimate the area/volume or the maximum width of the root system (Piñeros et al., 2016). The root cone angle proposed as the major indicator of root growth strategy (Alberda, 1953) is used very little. It can be described either by the outermost root (Grift et al., 2011; Courtois et al., 2013), by the dominant angles at 25%, 50%, 75% or 90% of the Root Tip Paths length (Das et al., 2015), or by the nodal root angles measured along an arc with a 10 cm radius from the middle of the stalk (Colombi et al., 2015).

In this paper, we describe the implementation and the features of the Rhizoscope-Analysis-Module, the software application we have developed to meet the requirements of CIRAD's high-throughput phenotyping platform. First, we present a new geometry modelling approach that consists to fit a "house-shaped" polygon on visual traits of the root system in order to characterize its ground penetration and soil exploration strategies. This polygon takes into account local root densities which allows to automatically discard non-significant points based on structure criteria and not from statistical methods as RANDOM SAmple Consensus (Das et al., 2015) or 95th percentile (Colombi et al., 2015). We then discuss the relevance of GT-RootS by statistically analysing two major but difficult-to-access parameters on a small-scale data set of about 30 rice root system images. This also makes it possible to demonstrate the image segmentation and characterization capabilities of GT-RootS. Lastly, we discuss the current limitations of the method and plans for further development.

2. Materials and methods

2.1. Root system phenotyping platform and plant materials

Rhizoscope is a high-throughput root system phenotyping platform for studying cereals (rice, barley, wheat and sorghum) and configured to manage up-to-30-days-old plants. It includes both a root growth unit and a root digitizing unit. The first unit is composed of several instrumented containers in which are immersed about two hundred two-

dimensional hydroponic-based systems called a rhizobox; the rhizobox is a sandwich of two 50 cm × 20 cm × 2 cm Plexiglas plates filled with glass beads that mimic soil resistance. Root growth can be examined, and quantitative parameters can be collected after removing the glass beads. A regular grid of cylindrical stainless steel pins is positioned in each rhizobox to hold the root system in place after bead removal. The second unit is an almost-dark room with a rigid frame on which are mounted a Nikon D810 camera coupled to a fixed focus lens (Nikkor 50 mm f/1.4 AF), a directional Siros-400-S Broncolor-light and a guide for vertically positioning the rhizobox in front of the camera. A strict digitizing protocol controls the directional-light intensity and the exposure time which ensures shooting standardization and allows automated image processing and phenotyping analysis. The 15-megapixel high-quality images are in JPEG format. In the high-throughput context, a software tool is needed to provide the balance between platform production capacity and the pace of numerical analyses.

The panel used in this study was composed of 35 cultivars of Japonica rice. The plants were grown in the hydroponic system of the Rhizoscope growth unit. After pre-germinating at 28 °C for three days, the well-developed seedlings were set on the top edge of the rhizoboxes. A modified Hoagland nutritive solution was circulated continuously through the rhizoboxes as described in (Roques et al., 2013). The solution pH was adjusted to and maintained at 5.4 ± 0.2 by automatic pH controllers. A cooling system maintained the temperature of the solution at 27 ± 1 °C. The conditions in the growth chamber were 28 °C during the day and 25 °C at night with a 12:12 photoperiod. The radiation was 400 to 450 μmol photons per m^2 per second. The relative humidity was set to 55%. After 30 days of growth, the rhizoboxes were taken out of the tanks, and the beads were removed. The whole root system, which remained in position on the nail plate, was photographed.

2.2. Procedure workflow

2.2.1. Image processing

The image processing step is designed to segment the root system, i.e. to define the root system silhouette by binary images in which root pixels are separated from background.

Segmentation includes several automated steps which gradually erase the noise and the non-root elements present in the rhizobox images as reflections, wear, scratches on the Plexiglas pane or retainer screws and Plexiglas pins. Images of different sizes are automatically processed without any user intervention, at a rate of 30 pictures per hour on a low-end computer (see below for details).

1. *Defining the Region of Interest* for which the pixel areas are strictly included in the Plexiglas box (see Figs. 1A & 5B). For this purpose, the original image is cropped from the pre-set positions and dimensions that were defined from the image of an empty rhizobox. Default cropping-box size is 2650×6500 pixels. This allows the process to consider, in particular, both the focal length of the camera and the distance between the camera and the rhizobox. The variations in the position of the successive rhizoboxes are sufficiently small to be considered as negligible. Nevertheless, the coordinates of the cropping box may be interactively adapted by the user if necessary.
2. *Colour-to-greyscale conversion* (see Fig. 1B). Colour-to-greyscale conversion seeks to significantly decrease both the amount of information that must be processed and the complexity of the segmentation algorithms that will be used. It must preserve the appearance and the discriminability of the original colour image. This is an open question still widely addressed (Wu and Toet, 2014; Jin and Ng, 2015). The usual methods seek to match the intensity, lightness, brightness or luminance of the grey image with the corresponding magnitude of the colour image (Kanan and Cottrell, 2012). Intensity is the simplest of the criteria used: it is defined by

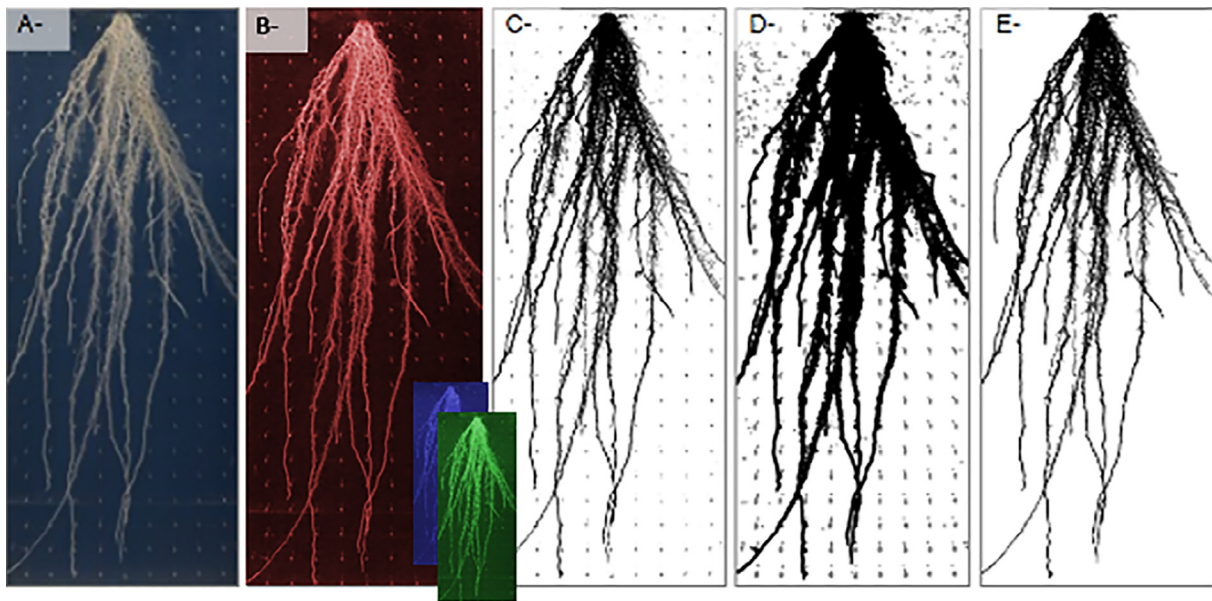


Fig. 1. Steps of the root system image processing pipeline. From left to right: A – Automated cropping of the original colour image (see Fig. 5B) from pre-set positions and dimensions; note that the decentring of the lighting source creates a heterogeneous background and various responses of the Plexiglas pins. B – The colour-to-grey conversion is to select the red channel that is systematically the most contrasted with a lot less noisy background. C – Binary image produced by Triangle thresholding; the outlines of the Plexiglas pins are more or less marked and distorted, and the root system is composed of several large components which are not connected. D – After application of a sized dilation, root components are reconnected and it becomes possible to label the different components of the root system. E – The resulting root system silhouette after removing the unlabelled components of the image. (For interpretation of the references to colour in this figure legend, the reader is referred to the web version of this article.)

the mean of the three red-green-blue channels. Luminance is often designated to match human perception by using a weighted combination of the red-green-blue channels. However, in the case of the Rhiscope digitizing unit, we find out that the roots reflect slightly more the red wavelength. The red channel is the most contrasted and systematically the lowest or the highest intensity of the three colour components. Of course, the user can choose another algorithm as one of the methods described above if better appropriate.

3. *Adaptive thresholding* (see Fig. 1C): a fixed-size window slides over the image and a threshold is computed for each position in order to binarize the image locally. The size of the sliding-window makes it possible to apply the threshold to a more or less large local neighbourhood and thereby absorb the strong variability of image intensities. Default size is pre-set to 285 pixels that is about 2 cm which corresponds to the spacing of the cylindrical pins stiffening the rhizobox, but the user can adapt this parameter if necessary. In (Tajima and Kato, 2011), the authors assess 16 different segmentation algorithms for the estimation of rice root length. For this, they compare automatic results with ones obtained by experts. According to this survey, the two best segmentation methods are the Triangle and Mean algorithms. Surový et al. (2014) present also a comparison of segmentation methods in the case of fine roots of woody plants. The authors conclude that the accuracy of the root area estimation depends significantly of the segmentation algorithm at the contrary of the root length estimation. In this second survey, the moment-preserving method appears to be the best segmentation method. In Colombi et al. (2015), the authors select the Otsu algorithm to segment automatically maize root systems in colour images.
4. *We can then conclude that* many different methods have been proposed to segment efficiently root systems and that, they depend both of the dataset and of the application. It is then difficult to draw a definitive conclusion about the best thresholding algorithm. However, in our application, we want to characterize the behaviour of the root system development that implies to find a global and robust segmentation of the roots which may be inaccurate for very

small structures. We propose then to use the Triangle method because it is well adapted to our root images that presents a unimodal intensity distribution (see Fig. 2). A straight line is then drawn from the maximum to the end of the histogram representation and the threshold is selected at the point of the histogram that maximizes the perpendicular distance between the straight line and the histogram (Zack et al., 1977; Rosin, 2001).

The key point of our approach is not the choice of the thresholding algorithm itself but the fact that the threshold value is computed locally in the image. This locally adaptive strategy allows to take into account the strong variability of the background of the Rhiscope images.

However, other threshold methods can be selected by the user (see the *advanced setting* dialogue box of the Fig. 5): (i) Intermodes method (Prewitt and Mendelsohn, 1966) where the threshold is the minimum value in bimodal or multimodal histogram, (ii) IsoData method (Ridler and Calvard, 1978) where the threshold is defined as the mean of the background and foreground averages, (iii) Mean method (Glasbey, 1993) where the threshold is the mean of the image grey levels, (iv) Moments Method (Tsai, 1985) where the threshold is deterministically defined in such a way that the moments of the input image is preserved in the binary image, and (v) Otsu method (Otsu, 1979) where the threshold minimizes the intra-class variance in a bimodal histogram.

5. *Root system enhancement*: A mathematical morphology operator called dilation is applied to the binary image in order to “connect” the close components potentially belonging to the root system (see Fig. 1D). We use a circular structuring element to expand the black components of the image. The circle radius is arbitrarily set to 1 mm. The root system (see Fig. 1E) is then defined by the intersection between the pre-segmented image and the largest component of the dilated image.

2.2.2. Global shape characterization

We introduce a house-shaped polygon for charactering the global shape of root systems that present a ground-penetrating angle before

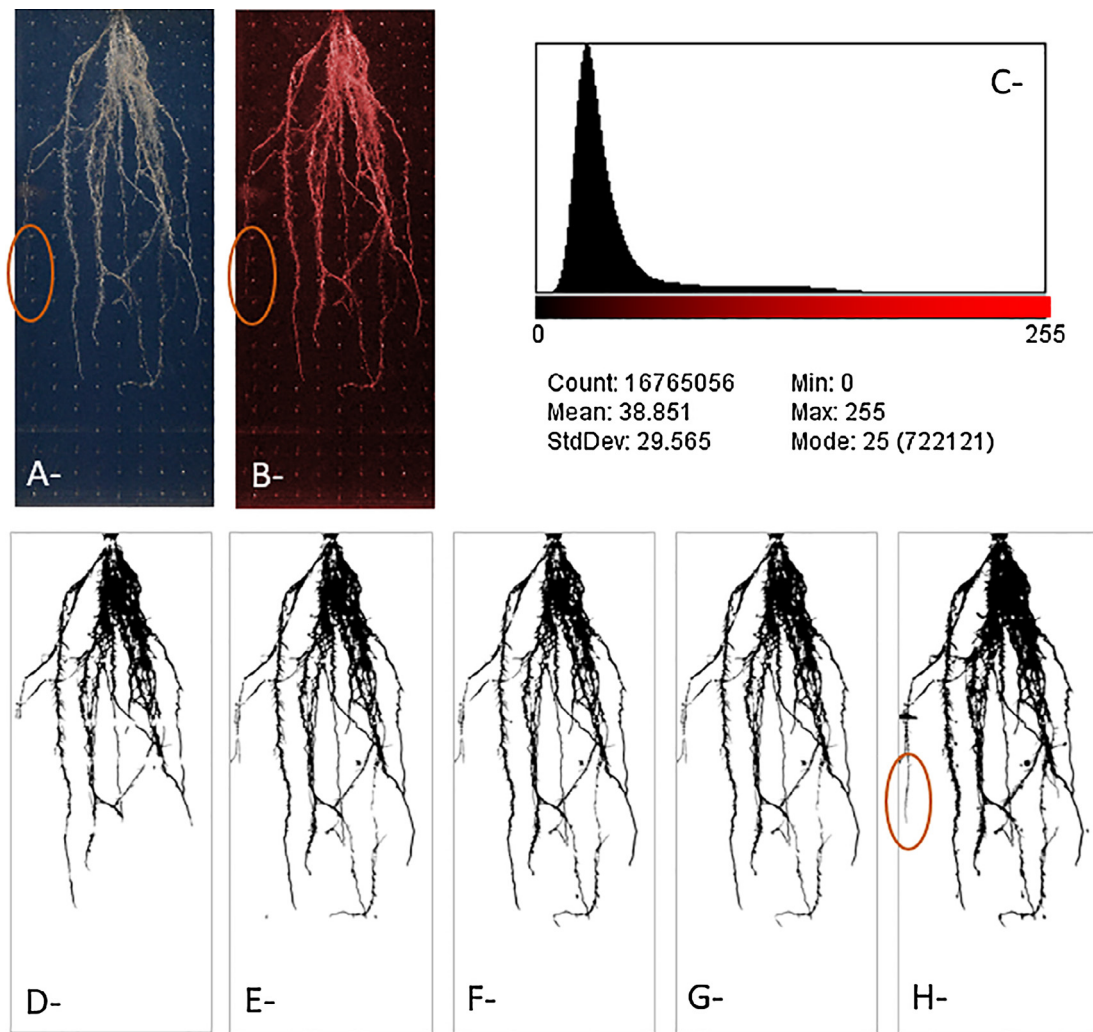
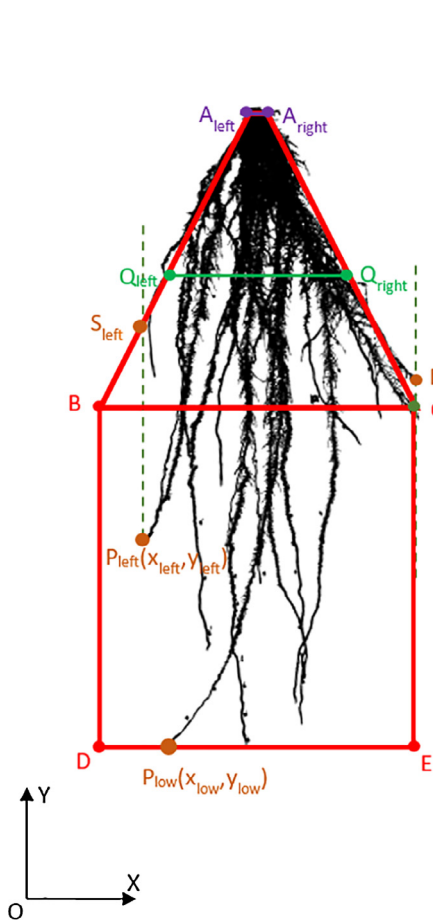


Fig. 2. Comparison of thresholding methods. A – The colour image of the root system. B – The red channel (coded on 8-bit) of the root system. C – The monomodal intensity histogram of the red channel, well suitable for the Triangle thresholding algorithm. D–H – Root system segmentation provided by the processing pipeline with respectively the Intermodes, IsoData, Moments, Otsu and Triangle algorithms. The Sorensen-Dice index, defined here by the ratio between the surface of the root system intersection and the surface of the root system union, quantifies the spatial similarity between two segmentations. On this sample, the mean similarity is 0.88% with a standard deviation of 0.06: the Triangle results are furthest from the others with a similarity index between 0.82 and 0.86%; but it is also the method giving as much detail as possible, especially on the background roots as pointed by the orange ellipse (and this tends to makes the image less similar to the others). In terms of global-shape, these results are visually identical: no matter what method segmentation occurs. (For interpretation of the references to colour in this figure legend, the reader is referred to the web version of this article.)

sinking vertically into the soil. This polygon is composed of two compartments: a trapezoid covering the upper part of the root system for the characterization of the ground penetrating and a rectangle covering the lower part for the characterization of the soil exploration. The covering polygon is defined as shown in Fig. 3 from both the coordinates of the four most external points and significant vertical weighted-density profiles of the root system. The weighted density describes the root system density according to its depth. Notice that this density is weighted by the local width of the system to give less emphasis to a single *very dense* root than to a complex *dense* root tangle. The weighted density at each depth d of the root system is defined by the harmonic mean providing the best combination of the two ratios r_1 and r_2 . r_1 is the d -horizontal root quantity compared to the d -horizontal root system width along the horizontal line defined by the direction of the minor axis of the root system ellipse; r_2 the d -horizontal root system width compared to an enough significant width pre-set here to 3 cm, i.e. 15% of the rhizobox width. Note that the modification of this reference value will affect the harmonic mean value but not its ranking. Two profiles of weighted densities are required to define the house-shaped polygon. The first profile is used to locate the top of the house-shaped

polygon. The top edge of the root system is defined by the minimum depth where the weighted density is greater than the limit between both the low-ratio and high-ratio classes resulting from 2-mean clustering. The second profile locates the densest horizontal zone of the root system: it is produced by setting the reference width with the greatest root system width. The densest depth of the root system is given by the minimum depth where the weighted density is maximum. The top edge and the densest zones are identified by their respective depth and represented by a horizontal segment corresponding to the local root system width. The extremities of these two segments define the left and right slopes of the upper trapezoidal compartment of the house-shaped polygon. The vertices of the polygon are obtained by geometrical intersections between the oblique lines of the upper trapezoidal compartment and the furthest-left, furthest-right and lowest edges of the lower rectangular compartment.

Notice that not all the points of the root system are necessarily included in the house-shaped polygon. Such a polygon gives the general shape of the root system without considering the local behaviour of the roots in the outlying area.



The root shape landmarks: the furthest-left, the furthest-right and the lowest points of the root system.

The root density landmarks: the left and right external points are defined using remarkable weighted-densities.

$A_{left}A_{right}$ is the minimum depth where the weighted-density is greater than the limit between both the low-ratio and high-ratio classes.

$Q_{left}Q_{right}$ is the minimum depth where the weighted-density is maximum

The built landmarks: the intersections between the left and right trapezoid slopes respectively defined from the density landmarks

P_{left} (resp. P_{right} and P_{low}) is the left-most (resp. right-most and lowest) point of the root system. Then,

$$S_{left} = [AQ]_{left} \cap X=x_{left} , S_{right} = [AQ]_{right} \cap X=x_{right}$$

The house-shaped polygon landmarks:

A_{left} & A_{right} : see above

B: ($X_{[AQ]_{left} \cap Y=y_B}$, $\min(Y_{S_{left}} , Y_{S_{right}})$)

C: ($X_{[AQ]_{right} \cap Y=y_C}$, $\min(Y_{S_{left}} , Y_{S_{right}})$)

D: (x_B , y_{low})

E: (x_C , y_{low})

Fig. 3. The root house-shaped polygon. The root system architecture may be defined by global shapes made of both trapezoids and rectangles: their respective vertices are based on noteworthy landmarks and significant weighted-density depths of the root system.

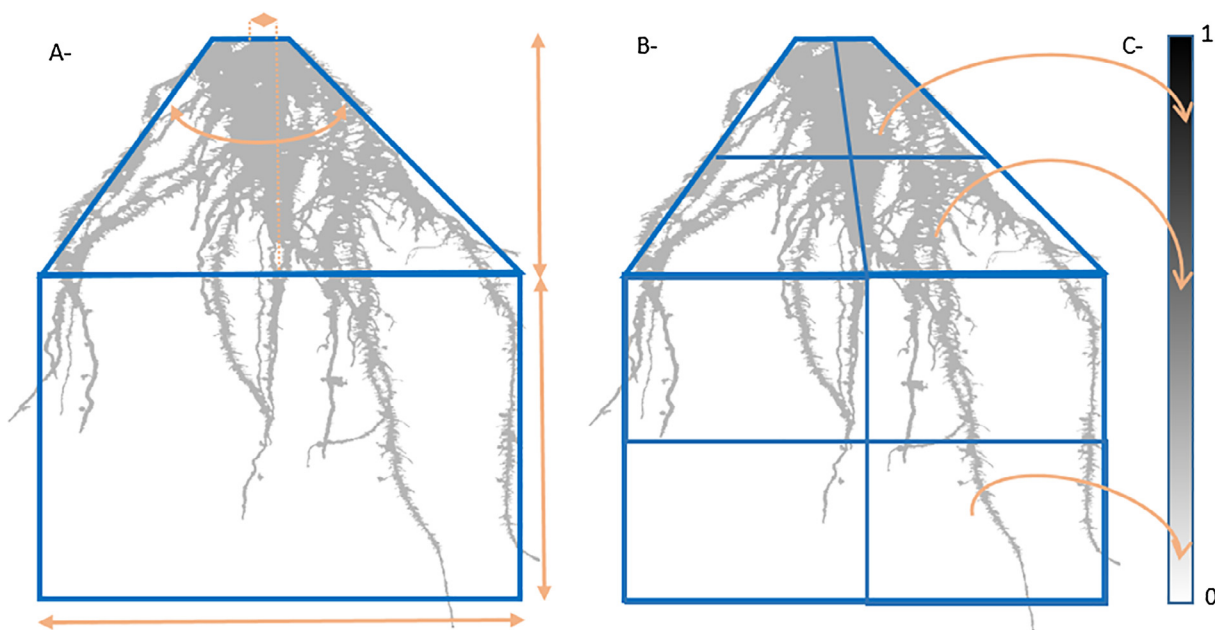


Fig. 4. Global trait estimation and root house-shaped polygon. A – The root house-shaped polygon enables an easy evaluation of geometry of the trapezoid and rectangular compartments (height, width and relative offset). B – Trapezoidal and rectangular compartments are subdivided into regions in which the root density is estimated by the ratio between the surface of the roots included in the region and surface of the region. These densities are localised into the house-shaped polygon.

2.2.3. Deep root characterization

The deep exploration ability of the plant can be characterized by the number of roots (Yoshida and Hasegawa, 1982) in the distal part of the root system. At this depth, the roots are “normally” well individualized.

We propose to model geometrically each root by its so-called skeleton, which is the line equidistant from the two boundaries (Abeysinghe et al., 2008). In image processing, the skeleton is usually computed by morphological thinning on a binary mask (Lee et al., 1994) which preserves the topology of the original image (Xie et al., 2003). The skeleton is then combined to a local distance computation (Borgefors, 1986; Thiel & Montanvert, 1992) which gives the shortest distance from the boundaries for each point of the skeleton. This distance gives a good diameter approximation of the detected roots.

Nevertheless, the density of the system prevents to individualize each root axis and to identify their connections. Geometrical information is not sufficient to give real descriptions about the root system structure as no root axes or no branching orders which could provide useful information about the nature or the orientation is identified. If we assume that the primary axes have diameters significantly greater than the secondary axes, we can differentiate the roots axes by defining a threshold on the diameter. We propose to define automatically an adaptive threshold by a 2-means algorithm and we will assess the validity of our assumption of diameter differentiation in Discussion section. Hence, there is no absolute size for the deep root counting, only a significant limit between two disjoint distributions of sizes. The deep roots should have diameters from about 1 mm as shown in Fig. 10.

GT-RootS is focused on simplified geometrical descriptors of dense cereal root systems for which it is hard to identify each root axis precisely. Global traits such as root width or cone angulation are estimated from the root house-shaped polygon as shown in Fig. 4.

For evaluating spatial root distribution, trapezoidal and rectangular compartments are subdivided into elementary areas (regular trapezes and rectangles, respectively) in which the root density is estimated by the ratio between the black and all-the-area pixels; the size of this decomposition is specified in the *spatial densities block* as shown in Fig. 5A. In the same way, vertical root density distribution is given from horizontal fixed-height bands. The density distribution is defined locally in the house-shaped polygon.

2.3. Graphical user interface

The GT-RootS graphical user interface (GUI) allows the end-user to easily calibrate and tune all the processing (see Fig. 5A). Image cropping, scale calibration and the deep scanning line can be defined either by numerical entries or by graphical adjustments.

Cropping is used to quickly exclude stickers and rhizobox walls. Scale calibration defines the pixel size in centimetres: the user adjusts the unit square of the pin grid on the graphical viewer and/or the centimetre correspondence on the *Calibration block* of the dialogue box. The deep scanning line specifies the absolute depth to the top edge of the cropping frame at which the deep roots are counted.

The Rhizoscope digitizing unit is based on a standardized protocol which guarantees the high similarity of the images produced. Pre-setting parameters are *a priori* valid for all the images (at least those from the same set). Nevertheless, the GUI allows the user to tune GT-RootS to process other plant species and images from another phenotyping procedure or platform.

Moreover, the GT-RootS GUI includes some management functionalities to select fully-automated or semi-automated processing (see Fig. 5A). The *compute-all* mode applies predefined standard processing to a set of images while the *compute-and-correct* mode is dedicated to the specific adaptation of some specific images. In practice, the second mode allows the user to indirectly modify the final results by manual corrections of the segmentation step result.

2.4. Output description

GT-RootS produces two types of results which are saved in the specified output folder. Firstly, numerical measurements are exported in a comma-separated-value file for statistical analysis: each line corresponds to a root system of the data set, and each column to an evaluated trait (see Table 1). Secondly, output images are produced to illustrate different steps of processing. For example, these images give the possibility to post check the root system segmentation or the house-shaped polygon construction (see Fig. 6A, B, D) or to display the density map (see Fig. 7C).

2.5. Software implementation

GT-RootS was developed in the Java language as a plugin for ImageJ, the Java-based open-source image processing program developed at the National Institutes of Health (Schneider et al., 2012). This plugin can be run on any Microsoft Windows, Mac OS or Linux computer with the 5.0 Java Virtual Machine (or later).

The core component of GT-RootS includes an automated Rhizoscope image processing pipeline, root system trait measurement and exporting of both numerical and visual results.

GT-RootS uses a light graphical user interface (GUI) to set scale calibration, select the input and output folders, and choose the usage modes: the fully-automated mode to process a set of Rhizoscope images, or the semi-automated mode to adapt standard processing to a specific image.

Software, data sets and a user guide can be downloaded from the http://amap-collaboratif.cirad.fr/pages-logiciels/?page_id=523 home page.

GT-RootS was developed under the free-software CeCILL licence which gives end-users the freedom to run, study, share, and modify software. See the official licence agreement http://www.cecill.info/licences/Licence_CeCILL_V2-en.html.

3. Results

3.1. Significant width and house-shaped polygon

The construction of the house-shaped polygon is based on two parameters: the threshold between the two weighted-density classes and the maximal weighted-density value. Nevertheless, the weighted densities depend on the value of the representative width. The variation of this width should have a significant impact on the contents of each density class. We evaluated the impact of this dependence on the geometrical parameters of the house-shaped polygon applying the image process pipeline to the data set with representative width of 3 and 6 cm. The mean variation of the main parameters are the following: 3% for the root cone angle (rca) (min = 0% – max = 9%), 1.5% for the house-shape surface (hA) (min = 0% – max = 6.5%), about 1% for the height (hH) and the width (hW) of the house-shaped polygon, 3.6% for the height of the trapezoid house-shaped compartment (upH) and about 2.5% of the rectangular house-shaped compartment (lowerH). These variations seem enough low and minor in a context of shape classification. However, they could be significantly stronger with another data set. We think the main issue is not to find the better width but to choose an enough representative width for the root shape comparison.

3.2. Analysis/assessment of experimental results

The output images offer the possibility of quickly appreciating the real relevance of the geometrical measurements, such as the root cone angle represented by the upper trapezoid of the house-shaped polygon. It can first be seen in Fig. 7 that root system diversity is very high, with different cultivars being used in each experiment.

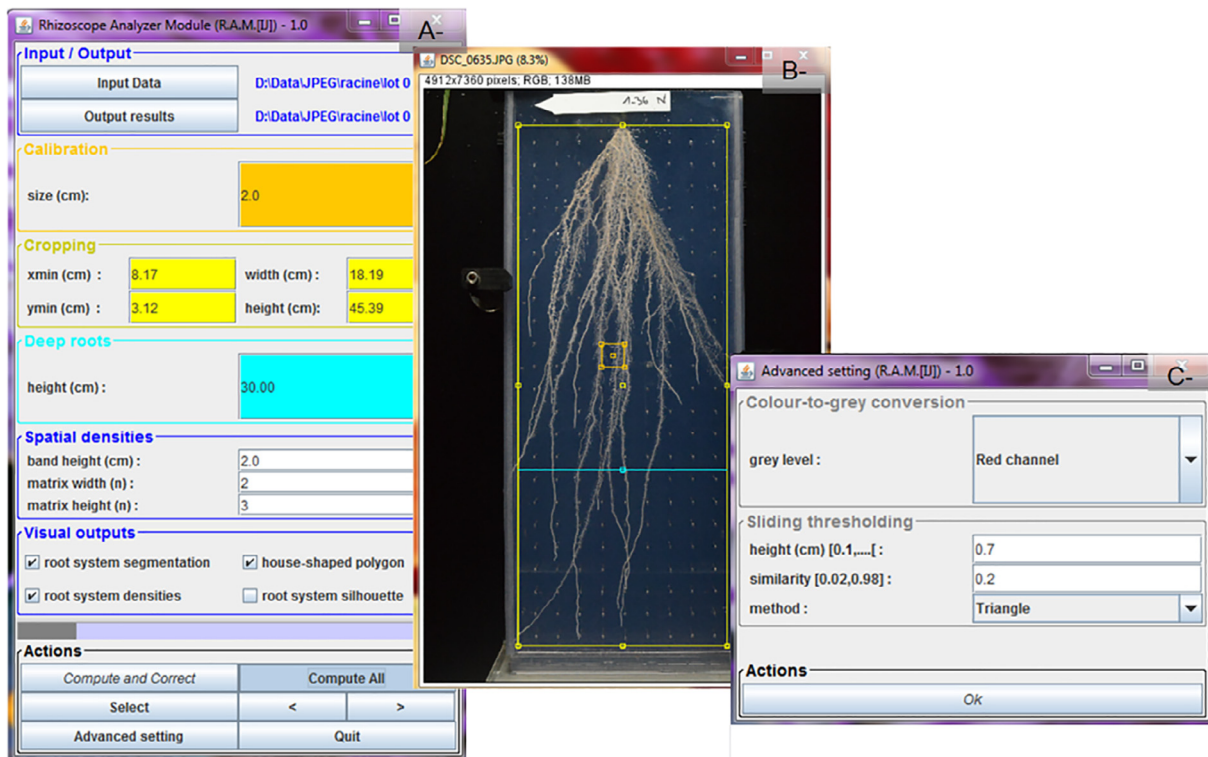


Fig. 5. The Graphical Interface User. User parameters (see Table 2) are set from either numerical inputs of the dialogue box (A-) or graphical adjustments in the image viewer (B-). The actions block (A-) allows the user to choose the interaction level and proposes some navigation functions in the input folder, especially for checking the inputs on several images or for selecting a specific image. The progress bar (in grey in the main dialogue box gives the processing status of the input folder).

Table 1
Trait description.

Trait	Units	Description
left Edge (lE)	y/n	Yes when the root system reaches the left side of the cropping box.
right Edge (rE)	y/n	Yes when the root system reaches the right side of the cropping box.
bottom Edge (bE)	y/n	Yes when the root system reaches the bottom of the cropping box.
root system deviation (α)	°	The angle between the major axis of the root system ellipse and the vertical edge of the cropping box. The value is positive for left inclination, and negative for right inclination of the root system.
house Area (hA)	cm ²	The area of the house-shaped polygon that covers the root system.
inside root Area (irA)	cm ²	The area of the root system which is inside the house-shaped polygon.
outside root Area (orA)	cm ²	The area of the root system which is outside the house-shaped polygon.
house Height (hH)	cm	The vertical difference between the upper and the lower edges of the house-shaped polygon.
house Width (hW)	cm	The horizontal difference between the furthest-left and the furthest-right edges of the house-shaped polygon.
root cone Angle (rca.)	°	The angle at the top point of the trapezoid house-shaped compartment.
upper Height (upH)	cm	The vertical difference between the upper and the lower edges of the trapezoid house-shaped compartment.
top Width (topW)	cm	The horizontal distance between the furthest-left and furthest-right top points of the trapezoid house-shaped compartment.
upper Offsett (upO)	cm	The horizontal distance between the middle point of the furthest-left and furthest-right extremities of the upper and lower edges of the trapezoid house-shaped compartment. The value is negative for the left offsets, and positive for the right offsets.
lower Height (lowerH)	cm	The vertical difference between the upper and the lower edges of the rectangular house-shaped compartment.
30 cm deep roots (N_{30cm})	n	The number of roots reaching the 30 cm depth as defined in (Courtois et al., 2013). This indicator can be zero for small root systems.
80% deep roots ($N_{80\%}$)	n	The number of roots reaching the 80% depth of the house-shaped polygon. This indicator can be zero for small root systems.
band Density (bandD _{t,h})	%	The percentage of the root surface in the polygonal area defined by the intersection between the house-shaped polygon and the horizontal band parameterized by its thickness t and its centre h.
upper Density (upD _{i,j})	%	The percentage of the root surface in the (i,j) trapezoidal area of the trapezoid house-shaped compartment. Trapezes result from the regular splitting of the trapezoidal house-shaped compartment.
lower Density (lowerD _{i,j})	%	The percentage of the root surface in the (i,j) rectangular area of the rectangular house-shaped compartment. Rectangles result from the regular splitting of the rectangular house-shaped compartment.

3.2.1. Error and interactive correction

Segmentation errors can be removed with the *compute-and-correct* mode where the user is invited to control and modify the result of the pre-segmentation stage. The most frequent errors are induced either by the low contrast of thin and background roots or by the scratches and deteriorations of the Plexiglas. The user can erase, thicken or connect certain parts of the binary pre-segmented image using the interactive

functions of ImageJ. Fig. 8 shows two typical cases: top, the area delineated by the orange contour is deleted by the eraser or the cutting function; bottom, thickening of the root part in the green ellipse will allow the root to be kept.

3.2.2. Relevance and repeatability of measurements

In order to demonstrate that the automated GT-RootS trait

Table 2
GUI description.

Block	Descriptive
Input/output	Allows the user to specify data and result folders
Calibration	Allows the user to set the size in centimetres of the pixel reference square
Cropping	Allows the user to numerically adjust the position and the dimension of the region of interest
Deep root	Allows the user to define the depth where roots will be individualized and counted
Spatial densities	Allows the user to specify the granularity of the spatial distribution of the root system densities: the vertical and house-shaped polygon splitting (see Fig. 6C) are defined by the dimension of the dividing grid splitting (see Fig. 5A), respectively
Visual outputs	allows the user to select the images which will be displayed during processing: by default, this will be <i>root system segmentation</i> , <i>house-shaped polygon</i> and <i>root system densities</i> . Moreover, the <i>root system silhouette</i> is proposed for additional measurements with another software such as DIRT (http://dirt.iplantcollaborative.org)
Colour-to-grey conversion	Allows the user to specify the method for the colour-to-greyscale conversion. The default method is based on the <i>Red channel</i> due to the spectral properties of the roots. The intensity defined by the <i>mean of the RGB channels</i> and the luminance defined by the <i>weighted combination of the RGB channels</i> are also available
Sliding thresholding	Allows the user to design (when necessary) the adaptive pre-segmentation by setting the height of the sliding window, the Dice threshold below which the compared clusters are considered as similar, and the intensity clustering method. The default is the <i>Triangle algorithm</i> well adapted to the monomodal distribution of intensities; the <i>Otsu and Moments-preserving algorithms</i> are available for grey images with a bimodal distribution

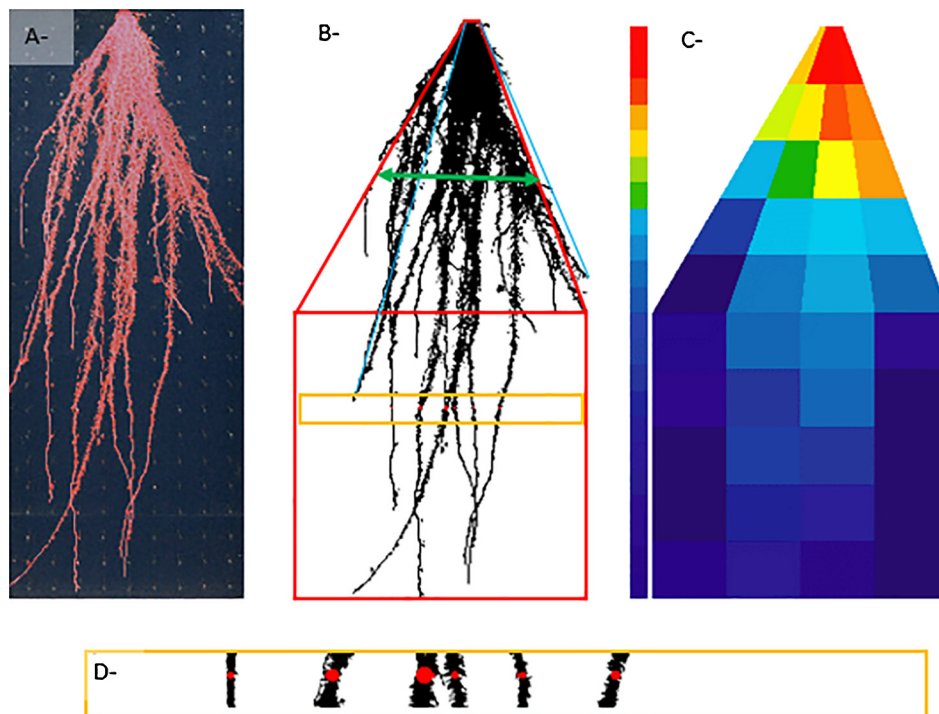


Fig. 6. The output images. A – Visual verification of segmentation accuracy: the segmented root system in red can be compared by transparency with the native image details. B – Visual verification of the root shape descriptor: the house-shaped polygon, in red, is superposed on the root silhouette, in black; the densest segment is drawn in green. Note that the house-shaped polygon can be larger than the image width. C – Spatial density distributions: on the left, vertical density distribution evaluated in each horizontal band; in the centre, density map from the 4×5 decomposition of the house-shaped polygon; on the right, density scale composed of 256 colours ranging from dark blue to bright red where the bright cyan corresponds to the mid-density. D – Magnification of the 30-cm-deep band allows visual control of the counted deep roots. They are represented by a red disk of the same diameter as the root. (For interpretation of the references to colour in this figure legend, the reader is referred to the web version of this article.)

estimation is well suited to high-throughput phenotyping analyses, it is necessary to assess the *repeatability, accuracy and relevance* of the GT-RootS estimators, especially on two hard-to-access parameters: root cone angulation and deep root number.

3.2.3. Root cone angulation

Firstly, we wanted to assess the difficulty of the task of clearly defining this trait in current practice. For this, we used a set of 32 Japonica rice root system images which we reversed left-to-right. Even if this data set is too small to give significant statistics, it illustrates the heterogeneity of the different cultivars and reflects some trends. These $2 \times 32 = 64$ images were presented to four eco-physiologists, familiar with measuring root system traits in digital colour images. They used the same measurement protocol based on a specific ImageJ plugin (see http://dev.mri.cnrs.fr/projects/imagej-macros/wiki/Root_Tools for more details). In Fig. 9A, the correlation can be seen between the results found in Dataset 1 (original image) and Dataset 2 (reversed image).

Then, we compared our GT-RootS RCA measurements with the experts' measurements as two automatic procedures:

- In (Courtois et al., 2013), RCA is defined between vertical and the furthest left and right crown roots (before roots reached the rhizobox sides and changed direction). We implemented Courtois's method by including angle computation in GT-RootS processing. The angular estimation was carried out in the axis system of the root ellipse for a more objective comparison of numerical estimations.
- DIRT software (Das et al., 2015) was also used in the comparative study. It proposes a root system trait close enough to our root cone angulation. In this software, the Root Top Angle is defined as the angle between the Random Sample Consensus (Fischler and Bolles, 1981) fit line at a 10% depth of the root system and the horizontal soil line. We thus used DIRT on our root system silhouette.

By evaluating the repeatability of the experts' measurements, it was possible to quantify the consistency of the experts and, indirectly, to best adjust the computation of the expected true-values by weighting each expert contribution differently. The weight associated with the measurement of a regular expert was greater than that of another more irregular expert. The mean intra-operator variability ranged from 0° to 30° depending on the experts; this attests the middle correlation shown

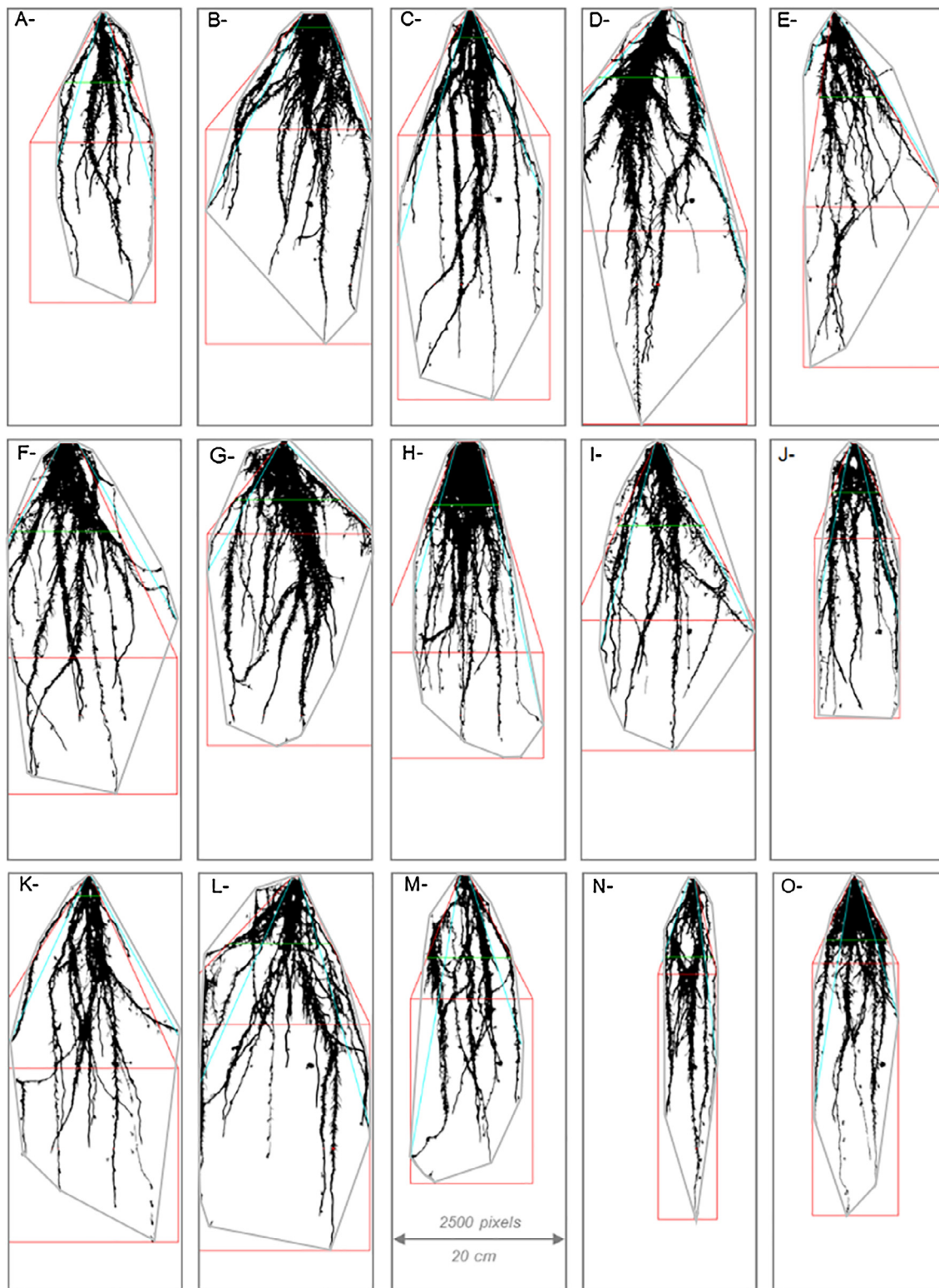


Fig. 7. House-shaped polygon and root system silhouette. Fifteen Japonica rice cultivars of the same Rhizoscope growth experiment: the root silhouette in black, the convex hull in grey, Courtois' root cone angle in cyan and the densest segment in green from which the house-shaped polygon in red was built. Note the relative offset between the trapezoidal and rectangular compartments, the outside roots, and the various ratios between the lower and the upper parts of the house-shaped polygon. (For interpretation of the references to colour in this figure legend, the reader is referred to the web version of this article.)

in Fig. 9A. Five regular variability classes were then built and a weighting coefficient on a scale of 1–5 was attributed to each expert. The true value was estimated for each expected angular measurement by weighting the mean, and its 68% confidence interval (1) was defined as a first approximation considering that the expert measurements

followed a normal distribution.

$$\left[\bar{x} - \frac{\sigma_x}{\sqrt{n}}, \bar{x} + \frac{\sigma_x}{\sqrt{n}} \right] \tag{1}$$

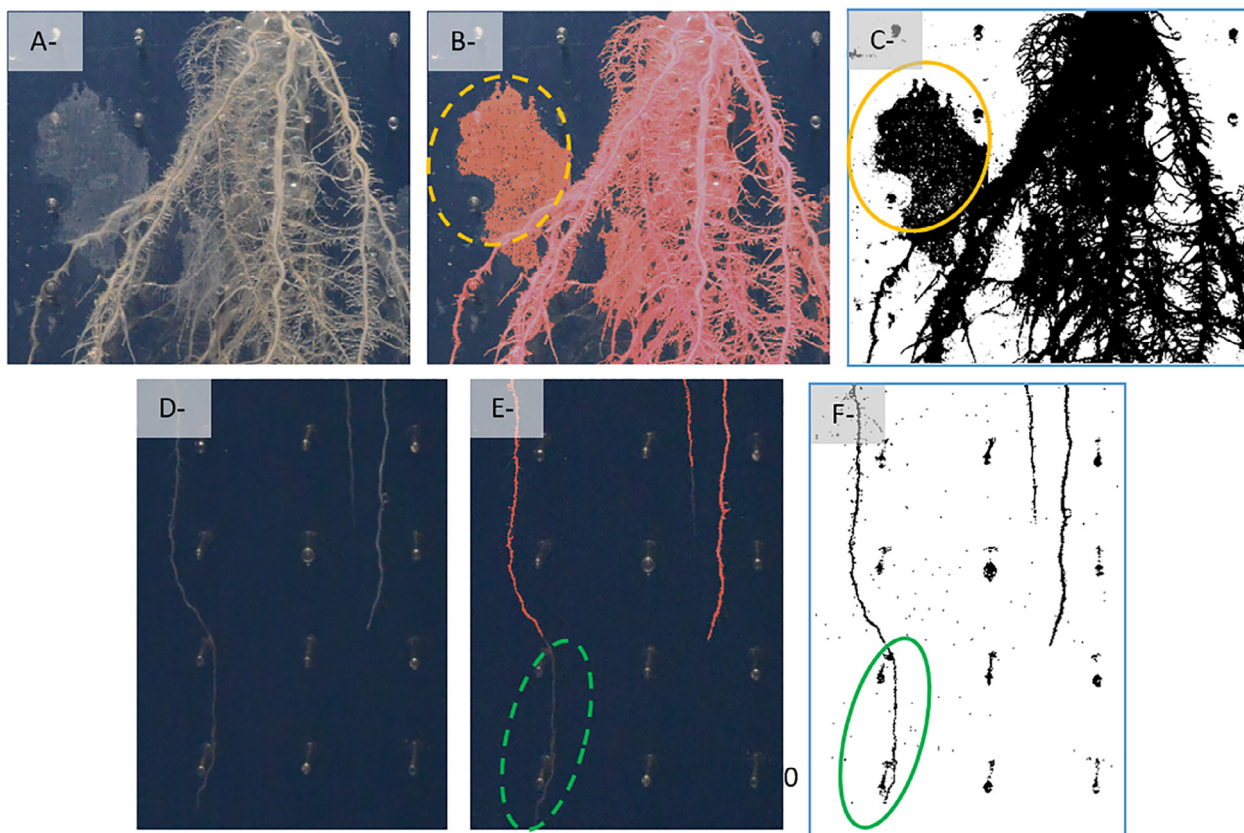


Fig. 8. Segmentation error and interactive correction. A – Original colour image. B – Output control image in which the segmented root system is superposed with transparency effects on the original image. C – The areas where the user can interact with the pre-segmentation results (see Fig. 1C).

where \bar{x} is the weighted mean, σ_x the standard deviation and n the number of weighted measurements.

Our own measurements were compared to both the mean expert true values and the similar automated measurements (*when it was possible*).

Nevertheless, the study of the expert RCA measurements highlighted the subjectivity of the current practice. The green series in Fig. 9A shows the mean intra-operator bias: here, the RCA values of the first dataset are compared to those of the second; they should be very close; but they present instead both a mean absolute error and a spread of about 10°. The coefficient of determination, 0.79, confirms that the angular measurements of the two datasets do not fit. The intra-expert variability is too high for deducing a significant confidence interval.

With an R^2 of 1.0, the automated RCA estimations are robust and repeatable.

Fig. 9B shows the crossed comparisons between the methods on the whole data. No correlation between methods was identified, as indicated by the low R^2 coefficients. Whatever the automated method considered, the angle measurements were mostly outside the 68% confidence interval (1). The mean angular error of GT-RootS, DIRT and Courtois methods with respect to the mean expert estimation were 9.9°, 13.3° and 18.5°, respectively. The errors of the Courtois and DIRT measurements with GT-RootS were 11.7° and 13.9°, respectively. These methods estimate the same parameter in different ways and are not really comparable. Each method is sensitive to another specific aspect. The expert estimation is based on the visual appreciation of the mean slope steepness of the two root crown sides; the angulation here is dependent on both the height and the peripheral density of the considered observation area. The Courtois angulation is evaluated from the external furthest left and furthest right points: a slight variation – or local noise – of the peripheral point positions may cause a major angular shift. The GT-RootS estimation is based on the global maximum of the

vertical density profile of the root system silhouette; it is less sensitive to both the uniform noise and the global variations of the root system shape. Moreover, the GT-RootS RCA is closest to the expected expert estimations with R^2 to 0.49 (0.44 for DIRT and 0.35 for Courtois).

3.2.4. Deep root number

The deep root number is another indicator which is difficult to automatize: while the experts identify and counted the primary deep roots by analysing the topology of the root system, the GT-RootS estimator used only a threshold on the diameter value to distinguish primary and secondary roots reaching a given depth.

In our experiments, we tried to assess both the reliability of the GT-RootS procedure and the automatic threshold computation.

For this, we used about fifty rhizobox images of rice root systems with varying plasticity. For each image, experts gave a representative point of each root reaching a depth of about 30 cm. We developed a specific module to compare the positions of the representative points given by the expert to the landmarks extracted by the GT-RootS counting procedure. For each image, a $P \times Q$ matrix of distances was introduced to define the closest match between the P expert points and the Q GT-RootS points: each expert point was matched with no more than one GT-RootS point (and conversely), and the matched points were as close as possible. Each pair formed in this way depended on a specific distance: infinity was assigned to the unmatched points. For each image we then evaluated the number of pairs in true positive (TP), false positive (FP) and false negative (FN) root classes according to a distance threshold and computed the precision (2), the recall (3) and the F-measure (Powers, 2011), which combines precision and recall to estimate the correlation between GT-RootS and expert counting. We were then able to analyse all these parameters with respect to the threshold on the diameter and obtain the curves presented in Fig. 10.

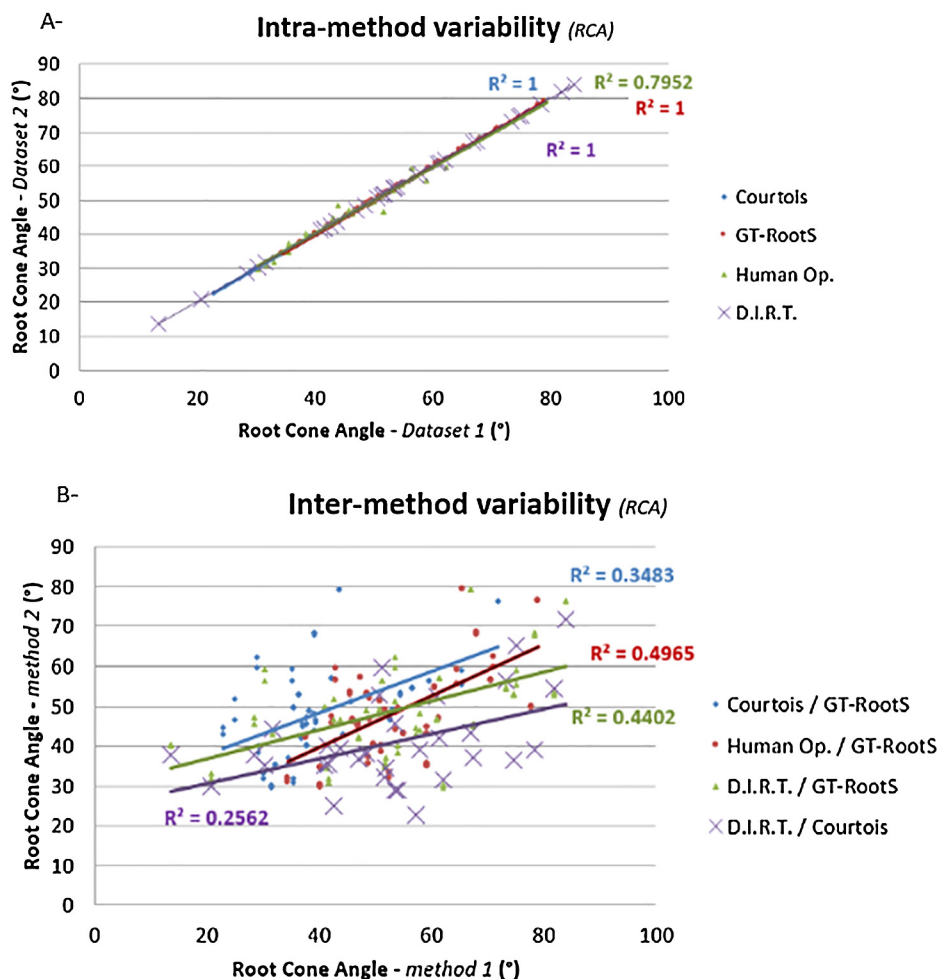


Fig. 9. Bias and variability of the root cone angle. A-: the intra-expert variability is a little high presumably due to the unconscious left-to-right image reading. B-: the crossed-method comparisons do not enable identification of significant correlations.

$$Precision_d = \frac{1}{n} \times \sum_{i=1}^n \frac{|TP|_{d,i}}{|TP|_{d,i} + |FP|_{d,i}} \quad (2)$$

$$Recall_d = \frac{1}{n} \times \sum_{i=1}^n \frac{|TP|_{d,i}}{|TP|_{d,i} + |FN|_{d,i}} \quad (3)$$

where d is the distance below which the matching between expert and automated root identification is considered as good, and n is the number of images in the data-set.

The F-measure (Powers, 2011) is the usual measurement that combines precision and recall. It is defined as the harmonic mean of precision and recall. This is approximately the average of the two indicators when they are close, and is more generally the square of the geometric mean divided by the arithmetic mean.

Fig. 10 shows the mean recall, precision and F-measure by classes of diameters evaluated from the 50 image dataset. We can see that the best diameter threshold – for which the F-measure value was maximum – is 0.357 mm with a F-measure value of 0.846. However, if we use the GT-RootS method using the adaptive diameter threshold described in the “Deep root characterization” section, we reach a F-measure of 0.896 which is somewhat better than the fixed threshold.

The study thus showed that the adaptive diameter threshold is the best option for the GT-RootS deep root estimator. This method leads to the best compromise between recall and precision in ensuring that the primary-secondary root threshold is adjusted to each case, i.e. each plasticity or each depth.

3.2.5. Numerical values

The following table presents some numerical results for the dense root systems shown in Fig. 7. The angular values of the compared methods do not seem linked. The other parameters describe the geometry (of the two compartments) of the house-shaped polygon (see Table 3).

The RCA values are largely outside the 68% confidence interval (1): this suggests that either the hypothesis of normal distribution is wrong or the estimations do not correspond to the same measurement. The differences introduced by authors to define root cone angulation explain the major numerical divergences. The supplementary parameters are given for information purposes only. Note that the root system depth or area presents a very good correlation with the expert or software measurements. These results are not presented in this paper as they are of no great interest.

3.2.6. Measurements and accuracy

A phenotyping study often needs both complex large-scale analyses and a broad range of measurements. The accuracy required for these analyses depends on the study objectives (and probably on the support of the study).

These measurements are used for identifying significant behaviours. But in absolute terms, a trend i.e. the manifestation of behaviour is not associated with the absolute accuracy of the measurements but rather with the match between the observable variation of the physiological phenomenon and the quantification of the observations. It is not the accuracy of the measurements which is the most important but the fact

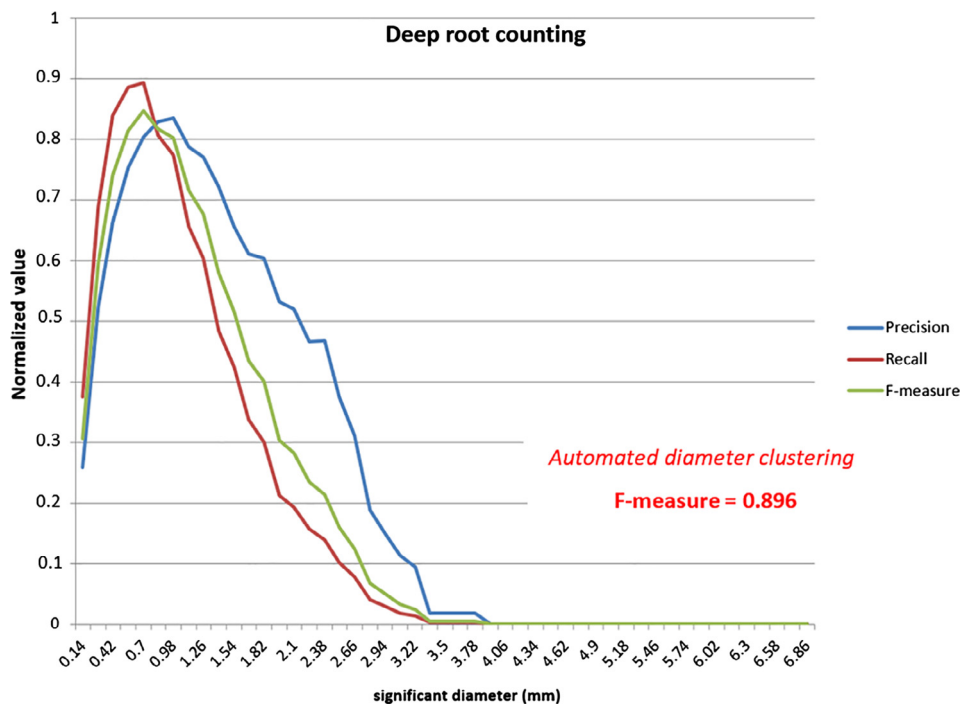


Fig. 10. Deep root counting. The Precision/Recall studies confirmed that the adaptive diameter thresholding is more efficient than the pre-fixed value to exclude secondary roots in the deep root counting step.

that the variation in the measurement indicates changed status. GT-RootS has been developed to facilitate the identification of trends. Three *internal rhizobox side* contact indicators are set to differentiate both the free and the constrained root system growths: these indicators guide the user in compiling homogeneous result sets for statistical studies.

Statistical classifiers (Ayodele, 2010) are usually used for identifying discriminatory traits or decision trees. However, GT-RootS quite easily avoids finding patterns from simple relative measurements. Fig. 11 illustrates how to use the relative heights and widths of the two house-shaped compartments to characterize root system spatial distribution.

4. Discussion

4.1. GT-RootS overview

This software was developed for high-throughput analyses and

satisfies the expected criteria.

1. *Speed*: the segmentation and measurement of the content of a colour image of 4912×7360 pixels takes about 2 min on a standard desktop (with a 3 GHz Xeon® W3550 processor).
2. *Full automation*: the user has just to specify the input and output folders, all the root system segmentation and parameter measurements are fully automated. Automation does not only increase the speed of the analysis but also eradicates any operator-dependency bias.
3. *Visual verification and adaptive correction*: user control is always possible from output images produced during root system processing. In the event of blatant anomalies, results can either be removed from further analysis or corrected by adapted reprocessing of the input image.
4. *Global measurement*: The characterization of dense cereal root systems for which it is hard to identify each root axis is made possible

Table 3
Examples.

Id.	RCA (°)				hA (cm ²)	irA (cm ²)	orA (cm ²)	hH (cm)	hW (cm)	upH (cm)	upO (cm)	lowerH (cm)
	GT-RootS	expert	Courtois	DIRT								
8.a	48.5	56.8	30.3	28.5	330.9	60	4.4	31.7	13.3	14.1	1.1	17.5
8.b	60.8	73	44.2	60.9	549.9	111.8	0.9	36.2	17.9	12.7	2.6	23.5
8.c	59	52.3	35.7	13.5	576.4	106.1	0.4	42.5	16	13.6	-0.4	28.9
8.d	60.4	53.8	54.1	73.3	1055.1	134.5	2	45.4	31.3	24.2	7.2	21.1
8.e	36.8	48.1	53.2	74.5	436.1	68	4.6	38.8	15.3	21.3	-4.3	17.6
8.f	52.4	63.7	55.3	75	690	113.3	7.3	38.4	25	23.5	1.1	14.9
8.g	80.4	72.3	71.9	84	497.9	126.1	4.6	33.1	17.6	9.9	-0.7	23.2
8.h	37.4	47.3	27.7	54	442.6	111.9	1.9	34.7	18	23.1	1.1	11.6
8.i	50.3	44.9	39.6	61.3	459	86.1	4	33.6	18.9	19.4	-0.6	14.2
8.j	43.2	53.7	23.6	42.6	228	68.6	3.2	30.1	9	10.4	-0.3	19.7
8.k	55.6	54.3	52.4	81.8	676.4	85.5	3.8	40	22.8	21	1.9	19
8.l	67.6	66.8	38.5	77.6	765.3	121.7	3.1	40.9	23.1	16.1	3.7	24.8
8.m	47.7	46.6	26.4	53.4	354.5	71.4	3.2	33.8	12.9	13.6	-0.7	20.2
8.n	30	42.4	24.1	41.6	204	56.9	3.4	37.3	6.3	10.5	0.5	26.8
8.o	48.9	54.7	24.6	67.4	296.4	73.9	1.1	36.8	9.1	9.2	-0.1	27.6

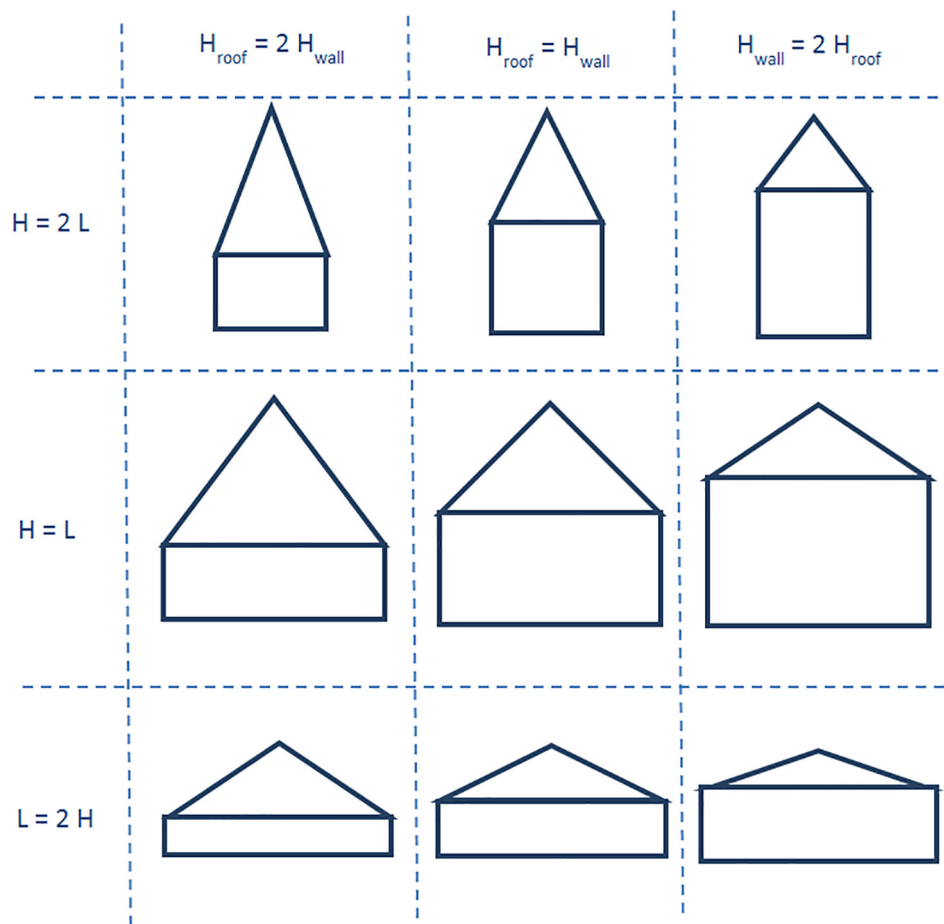


Fig. 11. Root system growth trends and the house-shaped polygon. The figure illustrates the shape classification from a single height and width ratio. In this case, the topW trait is negligible with respect to the hW trait – for example less than one tenth – , and the upper compartment is considered as triangular.

by the house-shaped polygon. This polygon defines the best covering shape from which some geometry and spatial density indicators can be estimated

4.2. Some limitations

The objective of GT-RootS is to improve and normalize high-throughput measurements from root system images produced by the rhizoscope digitizing unit. The limitations of the software are the direct consequences of the technical orientation dictated by this objective.

Firstly, GT-RootS does not include the ability to add complementary parameters to the automated measurement processing. Some additional measurements are however possible from the root system silhouette with the ImageJ measurement functionalities or another particular software such as DIRT.

Secondly, the processing pipeline has been designed for the specific images produced by the Rhizoscope digitizing unit. However, adaptations are still possible through the choice of other thresholding methods or the settings of the sliding band.

Thirdly, the Triangle algorithm is well-adapted for images composed of some light points – the root system points – and many dark points – the background points –, i.e. for strongly decentred monomodal intensity distribution; the Otsu algorithm can threshold images with pronounced bimodal distribution, i.e. images with a very dense root system. In the other configurations, the pre-segmented algorithms will be inefficient. Note we successfully tested the GT-RootS processing pipeline on rice root images from 6 genotypes downloadable from the Technology Georgia Institute home. The downloaded images presented colours slightly different from those of the rhizoscope images: light beige roots on a

homogeneous light blue background; the colour-to-greyscale conversion restored the required intensity conditions for more efficient automated Otsu clustering.

However, the GT-RootS objective is not to process digital images from various sources. We chose to limit human-machine interaction to suppress the bias induced by human appreciation. The produced results are truly comparable because they are rigorously generated from the same image processing pipeline, even in the case of the semi-automated mode.

Thresholds automatically computed from a statistical analysis of value distributions offer a reasonable alternative to thresholds arbitrarily set once by human users. They are easy to establish from a given numerical value set divided into two clusters by a specific classifier, even in the absence of significant differences. GT-RootS proposes an alternative to this major disadvantage. When their respective means are too close, the two clusters are merged; the kept cluster depends on the considered step. For the pre-segmentation step, the higher class is included with the lower and all the points are considered as belonging to the background. For deep root estimation, the lower class is included with the higher; all roots (of the higher cluster) are considered as primary. We use an adaptation of the Sorensen-Dice index (Dice, 1945) defined for comparing the similarity of two samples. The lower and higher classes of the respective m_i mean are considered as similar when

$$\frac{m_{higher} - m_{lower}}{m_{higher} + m_{lower}} < 0.2i. e. m_{higher} < 1.5 \times m_{lower} \tag{4}$$

4.3. Advantages of the house-shaped polygon

The house-shaped polygon reflects implicitly the strategy of the root system growth: its geometrical properties leads to a significant differentiation between the topsoil root systems and the deep root systems. The major interest of the covering polygon is to classify the root system behaviours based on a very little number of parameters: penetration angulation and root level heights. This reduced description is in opposition with the RSA approaches which are rather based on many accurate and fine measurements of the root axes (Kochian, 2016; Das et al., 2015) as mean or cumulated lengths, distribution of root diameters, and profile of root densities. These parameters characterize mainly the functional capability of the plant and not directly its growing strategy. Moreover, unlike our method, RSA approaches are limited to the study of scattered root systems as they are based on a structural decomposition of the root system.

Fig. 9 illustrates the difficulty to define the penetration angular. Several definitions have been proposed (Courtois et al., 2013; Das et al., 2015) but none is really adopted by the scientific community. Ours has the advantage to be easy to understand because it is directly defined from (the slopes of) the house-shaped polygon.

The house-shaped polygon is well-adapted in measuring the global feature of dense plant root system form. The parameters can be displayed on the root system which facilitates the validation or invalidation of numerical measures.

5. Conclusion and future work

This paper describes the automated Java-based open-source solution we are developing for processing root system images provided by the Rhizoscope, a CIRAD phenotyping platform dedicated to dense cereal plants. Two aspects are presented: the specific image processing pipeline and an original descriptor of the dense root system shape.

We introduce a shaped-house polygon for defining the type of the root system form and so the root growing strategy; this polygon is composed of two compartments: a trapezoid covering the upper part of the root system and a rectangle for the lower part. These compartments are mapped on the root system silhouette from directional density indicators.

The characterization of dense cereal root systems for which it is hard to identify each root axis is made possible by the house-shaped polygon. The global parameters/features of the root system form are evaluated from the main geometry and density properties of the covering polygon. Upper penetration angles or root densities were estimated for characterizing the plant strategy and ability of soil exploration. The major interest of the covering polygon is to characterize the root growing strategy and classify the root system behaviours from a very little number of parameters: penetration angulation and root level heights. This reduced description is in total opposition with the RSA approaches which are rather based on many accurate and fine measurements of the root axes as mean or cumulated lengths, distribution of root diameters, and profile of root densities. RSA parameters characterize mainly the functional capability of the plant and not directly its growing strategy. This geometry model could contribute to study the regenerative capacity of plants or the ground penetrating ability of root systems in the particular context of the climate change.

Experimental studies were just focused on the geometry-sensitivity of the house-shaped polygon. Several experimentations were realized using a representative set composed of about 32 Japonica rice root systems. We demonstrated that the major parameters were enough invariant to be used as signature of the root system.

GT-RootS is a dedicated image processing software for measuring both the global shape and the growth of rice root systems based on certain traits. It may probably be applicable to other root system shape. However, some extensions might be required to widen the scope of the phenotyping analysis.

Firstly, some other indicators should be introduced, especially the usual measurements of root axes: length and diameter classes and orders. This requires structural segmentation in which each root axis is identified. Back-tracking a root from its deepest level to its origin is possible and would make it possible to build the root system topology. Such information could significantly increase the accuracy of deep root counting, and perhaps address some questions about root architecture units (Jourdan and Rey, 1997) and about morphology and functioning aspects.

Secondly, house-shaped polygon definition could be extended to other strategies of root system developments. For example, in case of taproot systems that take rather the form of diamonds, we have proposed to use a double-quadrangle-shaped polygon (Borianne et al., 2016). Several weightings are possible to produce the vertical density profiles or identify density depths. A harmonic mean combining root area ratio and size shape ratio could be used to choose the best house-shaped polygon from many solutions, i.e. the smallest and most covering polygon.

Thirdly, in the Rhizoscope configuration, GT-RootS could be extended to study the juvenile stages of perennial plants with tap root systems such as cotton and eucalyptus, or fasciculate root systems such as palms. We have to adapt the root covering canonical shape (a house in our current application) to another form, such as a reversed house, diamond or hourglass shape.

Acknowledgement

We wish to thank Hervé Rey for its constructive exchanges about root system architecture, Mathilde Bettembourg, Sonia Mohamed and Sandrine Roques for their expert measurement work required for the comparative study, and Peter Biggins for his English language revision. Lastly, we should like to thank the reviewers for their detailed comments and suggestions for improving the paper. This work was carried out as part of the RoSoM project. This project is supported by Agropolis Fondation under reference ID 1202-073 through the “Investissements d’avenir” programme (Labex Agro: ANR-10-LABX-001-01).

References

- Abeysinghe, S.S., Baker, M., Chiu, W., Ju, T., 2008. Segmentation-free skeletonization of grayscale volumes for shape understanding. *IEEE Shape Model. Appl.* 63–71.
- Adu, M.O., Chatot, A., Wiesel, L., Bennett, M.J., Broadley, M.R., White, P.J., Dupuy, L.X., 2014. A scanner system for high-resolution quantification of variation in root growth dynamics of Brassica rapa genotypes. *J. Exp. Bot.* eru048.
- Alberda, T., 1953. Growth and root development of lowland rice and its relation to oxygen supply. *Plant Soil* 5 (1), 1–28.
- Araus, J.L., Cairns, J.E., 2014. Field high-throughput phenotyping: the new crop breeding frontier. *Trends Plant Sci.* 19 (1), 52–61.
- Armengaud, P., Zambaux, K., Hills, A., Sulpice, R., Pattison, R.J., Blatt, M.R., Amtmann, A., 2009. EZ-Rhizo: integrated software for the fast and accurate measurement of root system architecture. *Plant J.* 57 (5), 945–956.
- Audebert, A., Ghneim, T., Roques, S., Thaunay, P., Fleuriot, J.P., 2010. Development of a high-throughput system for phenotyping rice root traits. In: The 28th International Rice Research Conference, 8–12 November 2010, Hanoi, Vietnam, OP11: Harnessing Biodiversity.
- Ayodele, T.O., 2010. Introduction to Machine Learning. INTECH Open Access Publisher.
- Borgefors, G., 1986. Distance transformations in digital images. *Comput. Vis. Graph. Image Process.* 34 (3), 344–371.
- Borianne, P., Subsol, G., Audebert, A., 2016. Automated characterization of the mature root system form by a double-quadrangle-shaped polygon. In: Functional-Structural Plant Growth Modeling, Simulation, Visualization and Applications (FSPMA), IEEE International Conference on, 6–15.
- Brewer, M.T., Lang, L., Fujimura, K., Dujmovic, N., Gray, S., van der Knaap, E., 2006. Development of a controlled vocabulary and software application to analyze fruit shape variation in tomato and other plant species. *Plant Physiol.* 141 (1), 15–25.
- Clark, R.T., Famoso, A.N., Zhao, K., Shaff, J.E., Craft, E.J., Bustamante, C.D., Mccouch, S.R., Aneshansley, D.J., Kochian, L.V., 2013. High-throughput two-dimensional root system phenotyping platform facilitates genetic analysis of root growth and development. *Plant, Cell Environ.* 36 (2), 454–466.
- Colombi, T., Kirchgessner, N., Le Marié, C.A., York, L.M., Lynch, J.P., Hund, A., 2015. Next generation shovelomics: set up a tent and REST. *Plant Soil* 388 (1–2), 1–20.
- Comas, L.H., Becker, S.R., Von Mark, V.C., Byrne, P.F., Dierig, D.A., 2014. Root traits contributing to plant productivity under drought. *Ecophysiology of root systems-environment interaction*, 18.

- Courtois, B., Audebert, A., Dardou, A., Roques, S., Ghneim-Herrera, T., Droc, G., Frouin, J., Rouan, L., Goz , E., Kilia, A., Ahmadi, N., Dingkuhn, M., 2013. Genome-wide association mapping of root traits in a japonica rice panel. *PLoS ONE* 8 (11), e78037. <http://dx.doi.org/10.1371/journal.pone.0078037>.
- Das, A., Schneider, H., Burridge, J., Ascanio, A.K.M., Wojciechowski, T., Topp, C.N., Lynch, J.P., Weitz, J.S., Bucksch, A., 2015. Digital imaging of root traits (DIRT): a high-throughput computing and collaboration platform for field-based root phenomics. *Plant Methods* 11 (1), 1.
- Dice, L.R., 1945. Measures of the amount of ecologic association between species. *Ecology* 26 (3), 297–302.
- Fischler, M.A., Bolles, R.C., 1981. Random sample consensus: a paradigm for model fitting with applications to image analysis and automated cartography. *Commun. ACM* 24 (6), 381–395.
- Galkovskiy, T., Mileyo, Y., Bucksch, A., Moore, B., Symonova, O., Price, C.A., Topp, C.N., Iyer-Pascuzzi, A.S., Zurek, P.R., Fang, S., Harer, J., Benfey, P.N., Weitz, J.S., 2012. GiA Roots: software for the high throughput analysis of plant root system architecture. *BMC Plant Biol.* 12 (1), 116.
- Glasbey, C.A., 1993. An analysis of histogram-based thresholding algorithms, CVGIP. *Graph. Models Image Process.* 55, 532–537.
- Granier, C., Vile, D., 2014. Phenotyping and beyond: modelling the relationships between traits. *Curr. Opin. Plant Biol.* 18, 96–102.
- Gregory, P.J., Bengough, A.G., Grinev, D., Schmidt, S., Thomas, W.B.T., Wojciechowski, T., Young, I.M., 2009. Root phenomics of crops: opportunities and challenges. *Funct. Plant Biol.* 36 (11), 922–929.
- Grift, T.E., Novais, J., Bohn, M., 2011. High-throughput phenotyping technology for maize roots. *Biosyst. Eng.* 110, 40–48.
- Humlplk, J.F., Laz r, D., Husi kova, A., Spichal, L., 2015. Automated phenotyping of plant shoots using imaging methods for analysis of plant stress responses—a review. *Plant Methods* 11 (1), 1.
- Iyer-Pascuzzi, A.S., Symonova, O., Mileyo, Y., Hao, Y., Belcher, H., Harer, J., Weitz, J.S., Benfey, P.N., 2010. Imaging and analysis platform for automatic phenotyping and trait ranking of plant root systems. *Plant Physiol.* 152 (3), 1148–1157.
- Jin, Z., Ng, M.K., 2015. A contrast maximization method for color-to-grayscale conversion. *Multidimension. Syst. Signal Process.* 26 (3), 869–877.
- Jourdan, C., Rey, H., 1997. Architecture and development of the oil-palm (*Elaeis guineensis* Jacq.) root system. *Plant Soil* 189 (1), 33–48.
- Kanan, C., Cottrell, G.W., 2012. Color-to-grayscale: does the method matter in image recognition? *PLoS one* 7 (1), e29740.
- Kochian, L.V., 2016. Root architecture. *J. Integr. Plant Biol.*
- Kuijken, R.C., van Eeuwijk, F.A., Marcelis, L.F., Bouwmeester, H.J., 2015. Root phenotyping: from component trait in the lab to breeding. *J. Exp. Bot.* 66 (18), 5389–5401.
- Lee, T.C., Kashyap, R.L., Chu, C.N., 1994. Building skeleton models via 3-D medial surface axis thinning algorithms. *CVGIP. Graph. Models Image Process.* 56 (6), 462–478.
- Lesk, C., Rowhani, P., Ramankutty, N., 2016. Influence of extreme weather disasters on global crop production. *Nature* 529 (7584), 84–87.
- Li, L., Zhang, Q., Huang, D., 2014. A review of imaging techniques for plant phenotyping. *Sensors* 14 (11), 20078–20111.
- Lynch, J., 1995. Root architecture and plant productivity. *Plant Physiol.* 109, 7–13. 10.1104/pp.109.1.7.
- Mathieu, L., Lobet, G., Tocquin, P., P rilleux, C., 2015. “Rhizoponics”: a novel hydroponic rhizotron for root system analyses on mature *Arabidopsis thaliana* plants. *Plant Methods* 11 (1), 3.
- Otsu, N., 1979. A threshold selection method from grey scale histogram. *IEEE Trans. Syst. Man Cyber.* 1, 62–66.
- Pace, J., Lee, N., Naik, H.S., Ganapathysubramanian, B., L bberstedt, T., 2014. Analysis of maize (*Zea mays* L.) seedling roots with the high-throughput image analysis tool ARIA (Automatic Root Image Analysis). *Plos One.* 10.1371/journal.pone.0108255 M.L.
- Parry, M.L., Rosenzweig, C., Iglesias, A., Livermore, M., Fische, G., 2004. Effects of climate change on global food production under SRES emissions and socio-economic scenarios. *Global Environ. Change* 14 (1), 53–67.
- Prewitt, J.M.S., Mendelsohn, M.L., 1966. The analysis of cell images. *Ann. N. Y. Acad. Sci.* 128, 1035–1053.
- Pi eros, M.A., Larson, B.G., Shaff, J.E., Schneider, D.J., Falco, A.X., Yuan, L., Shaw, N.M., 2016. Evolving technologies for growing, imaging and analyzing 3D root system architecture of crop plants. *J. Integr. Plant Biol.* 58 (3), 230–241.
- Pound, M.P., French, A.P., Atkinson, J.A., Wells, D.M., Bennett, M.J., Pridmore, T., 2013. RootNav: navigating images of complex root architectures. *Plant Physiol.* 162 (4), 1802–1814.
- Powers, D.M., 2011. Evaluation: from precision, recall and F-measure to ROC, informedness, markedness and correlation. *J. Mach. Learn. Technol.* 2 (1), 37–63.
- Rellan-lvarez, R., Lobet, G., Lindner, H., Pradier, P.L., Sebastian, J., Yee, M.C., Geng, Y., Trontin, C., LaRue, T., Schragger-Lavelle, A., Haney, C.H., Nieu, R., Maloof, J., Vogel, J.P., Dinneny, J.R., 2015. GLO-Roots: an imaging platform enabling multi-dimensional characterization of soil-grown root systems. *Elife* 4, e07597.
- Ridler, T.W., Calvard, S., 1978. Picture thresholding using an iterative selection method. *IEEE Trans. Syst. Man Cybernet.* 8, 630–632.
- Ristova, D., Rosas, U., Krouk, G., Ruffel, S., Birnbaum, K.D., Coruzzi, G.M., 2013. RootScape: a landmark-based system for rapid screening of root architecture in *Arabidopsis*. *Plant Physiol.* 161 (3), 1086–1096.
- Roques, S., Dardou, A., Fleuriot, J.P., Thauunay, P., & Audebert, A., 2013. Notice d'utilisation du Rhizoscope: un outil de ph notypage racinaire. *Agritrop CIRAD* – <http://agritrop.cirad.fr/569641/> (French).
- Rosin, P.L., 2001. Unimodal thresholding. *Pattern Recogn.* 34 (11), 2083–2096.
- Schneider, C.A., Rasband, W.S., Eliceiri, K.W., 2012. NIH Image to ImageJ: 25 years of image analysis. *Nat. Methods* 9 (7), 671–675.
- Skirycz, A., Vandenbroucke, K., Clauw, P., Maleux, K., De Meyer, B., Dhondt, S., Pucci, A., Gonzalez, N., Hoebrechts, F., Tognetti, V.B., Galbiati, M., Tonelli, C., Van Breusegem, F., Vuylsteke, M., Inz , D., 2011. Survival and growth of *Arabidopsis* plants given limited water are not equal. *Nature Biotechnol.* 29 (3), 212–214.
- Surovy, P., Dinis, C., Maru ak, R., de Almeida Ribeiro, N., 2014. Importance of automatic threshold for image segmentation for accurate measurement of fine roots of woody plants. *Lesnický Casopis. For. J.* 60 (4), 244–249. <http://dx.doi.org/10.1515/forj-2015-0007>.
- Tajima, R., Kato, Y., 2011. Comparison of threshold algorithms for automatic image processing of rice roots using freeware ImageJ. *Field Crops Res.* 121 (3), 460–463.
- Thiel, E., Montanvert, A., 1992. Chamfer masks: discrete distance functions, geometrical properties and optimization. In: *Pattern Recognition, 1992. Vol. III. Conference C: Image, Speech and Signal Analysis, Proceedings., 11th IAPR International Conference on. IEEE*, pp. 244–247.
- Tisn , S., Serrand, Y., Bach, L., Gilbault, E., Ben Ameer, R., Balasse, H., Chareyron, G., 2013. Phenoscope: an automated large-scale phenotyping platform offering high spatial homogeneity. *Plant J.* 74 (3), 534–544.
- Tsai, W., 1985. Moment-preserving thresholding: a new approach. *Comput. Vis. Graph. Image Process.* 29, 377–393.
- Wang, L., Uilecan, I.V., Assadi, A.H., Kozmik, C.A., Spalding, E.P., 2009. HYPOTrace: image analysis software for measuring hypocotyl growth and shape demonstrated on *Arabidopsis* seedlings undergoing photomorphogenesis. *Plant Physiol.* 149 (4), 1632–1637.
- Wu, T., Toet, A., 2014. Color-to-grayscale conversion through weighted multiresolution channel fusion. *J. Electron. Imag.* 23 (4), 043004.
- Xie, W., Thompson, R.P., Perucchio, R., 2003. A topology-preserving parallel 3D thinning algorithm for extracting the curve skeleton. *Pattern Recogn.* 36 (7), 1529–1544.
- Yoshida, S., & Hasegawa, S., 1982. The rice root system: its development and function. Drought resistance in crops with emphasis on rice, 10.
- Zack, G.W., Rogers, W.E., Latt, S.A., 1977. Automatic measurement of sister chromatid exchange frequency. *J. Histochem. Cytochem.* 25 (7), 741–753.